Development of Long Range Based Railway Crossing Security Tools (PJL)

[1]Syifa Meiliana Hasna, [2*]Mila Kusumawardani, [3]Lis Diana Mustafa

[1]Digital Telecommunication Network Study Program, Department of Electrical Engineering, State Polytechnic of Malang, 65141, Indonesia.
[2,3]Telecommunication Engineering Study Program, Department of Electrical Engineering, State Polytechnic of Malang, 65141, Indonesia.
[1] syifahasna26@gmail.com , [2] mila.kusumawardani@polinema.ac.id, [3] lis.diana@polinema.ac.id

Abstract **—A railroad crossing is an intersection between a railway track and a road for motor vehicles. At guarded crossings, a flashing unit operates the gate lights and warning speakers, while officers record train arrival and departure times. However, data from UPT Sintelis Daop 8 Surabaya shows that this device often malfunctions, encouraging the development of a new monitoring and control system. The proposed system consists of node and server devices. The node, installed at the PJL post, includes a LoRa Ray module, relay, amplifier, LED light, speaker, push button, and vibration sensor. The server, installed at the Gubeng Surabaya station resort office, uses LoRa Ray and NodeMCU8266. When a train approaches, the push button activates the speaker and LED warning light. After the train passes, vibration data is detected, processed by LoRa Ray RX, transmitted to the LoRa receiver, and sent to a web server via Wi-Fi. Testing was conducted statically using vibrating objects at distances of 5–35 cm and directly at PT KAI DAOP 8 Surabaya. LoRa testing reached a maximum range of 760 meters. The system achieved excellent TIPHON results, with packet loss of 4 and delay of 80.38922 ms.**

Keywords — Delay, Lora Ray, Mikrokontroller, Module SW-420 Vibration Sensor, Nodemcu ESP8266, Packet Loss

I. INTRODUCTION

A railroad crossing is an intersection between a railway track and a motorized roadway, such as a highway, or a pedestrian path. These crossings are commonly found in urban areas, although they may also exist in rural areas. In general, railroad crossings can be classified into level crossings and non-level crossings. A level crossing refers to an intersection where a railway line and a road meet at the same elevation, while a non-level crossing refers to a separated crossing, such as a flyover or underpass. All types of crossings are equipped with safety systems to prevent accidents [1].

Each railroad crossing is supported by a guard post that operates for 24 hours. The post is equipped with a system used to operate the crossing gate, known as the flashing unit [2]. This device controls the crossing gate lights and warning speaker, while the guard post officer manually records the arrival and departure times of trains. The flashing unit consists of several components, including SCR, TDA with cooling systems, capacitors, relays, and VR. According to instrument damage data from UPT Sintelis Daop 8 Surabaya, this device frequently experiences failures [3].

Information from the head of UPT Sintelis Daop 8 Surabaya indicates that, within one year, an average of three to four flashing unit devices are damaged. These failures are caused by several factors, including broken lines, dirty lines [4], damaged components, loose component installation, and short circuits that may require total replacement of all components [5]. Such damage can disrupt the working process of PJL officers.

UPT Sintelis has handled flashing unit damage through several procedures [6]. First, the device is tested to identify the type of damage. Second, the cause of the failure is analyzed, followed by disassembly for further inspection. Third, repair planning is conducted after the damaged part has been located. Fourth, repair implementation is carried out according to the identified damage. Fifth, evaluation is performed by rechecking the device before testing and reassembling all components. Sixth, the device undergoes testing and functional observation. Finally, documentation is prepared for recapitulation purposes [7].

Further information from the head of UPT Sintelis Daop 8 Surabaya shows that the repair process is often constrained by the limited availability of components [8]. On average, only two to three instruments can be repaired each month [9]. This number is not proportional to the average number of damaged devices received. Therefore, additional components are required to support the repair process more effectively [10].

Previous research conducted by Electrical Engineering student Mohamad Ilham Syafrizal and colleagues, entitled "Monitoring System for Detection of Train Arrival Direction Based on the Internet of Things," discussed a similar system. The controlled system crossing gate lights and warning speakers, while also recording train arrival and departure times automatically using NRF24L01 LoRa antenna media. The study showed that the maximum antenna coverage was 250 meters, and the success of data transmission was influenced by the antenna placement at the research location [11].

Considering the problems described above, it is necessary to develop a new system that can simplify the repair process while maintaining the same main functions. The proposed system can also send information automatically to a web server, allowing station officers and PJL officers to access train arrival and departure data more easily. This feature is expected to support officers in recording train movement times more efficiently. The system uses the SW-420 vibration sensor module as a train

*Corresponding Author
E-ISSN: 2654-6531 P-ISSN: 2407-0807

arrival detector, Arduino Uno as the main controller, the LoRa Ray module as the communication medium, and an accumulator as the main power source. The system output consists of lights, speakers, and train arrival and departure time information displayed on the web server.

To ensure a comprehensive evaluation of communication reliability, this research also incorporates Quality of Service (QoS) analysis. As a standardized framework for measuring network performance, QoS is used to evaluate how effectively the system delivers data by examining critical parameters such as speed, reliability, and latency [13]. The main objective of this testing is to assess network stability through systematic calculations and observations [14]. Since environmental conditions and network traffic may vary throughout the day, data collection is conducted across four different time intervals: morning, afternoon, evening, and night. This multi-temporal testing approach is important to identify possible degradation in network quality caused by atmospheric conditions or daily interference patterns [15]. By observing system performance across different periods, this study provides a more robust and holistic representation of LoRa network consistency and its ability to maintain data integrity under various operational conditions.

II. METHODS

A. Research Stages

This research will discuss the Development of Long Range Based Railway Crossing Security Tools (PJL) (Case Study PT. KAI DAOP 8 Surabaya, Gubeng Station). The first thing to do is a literature study of some of the archives of PT. KAI DAOP 8 Surabaya Gubeng stations, supporting journals, related books or articles that have been published by various sources regarding security tools maintenance, and LoRa Communication that will be used in designing this system. In the second stage, system planning was carried out including hardware design with a system for reading time of train as well as application web design with *real-time* monitoring. The third stage is to design the system according to the concept. The fourth stage is system integration, namely connecting hardware devices with application web, so monitoring can be done in real time. The fifth stage is testing the system by trying the system that has been made. Then analyze the results of testing the tool. The next stage is the conclusions and suggestions of the research that has been done. The final stage is preparing a report that is used as evidence that this research has been carried out.

B. Block Diagrams

The diagram illustrates the sequential flow of data, starting from the sensor input to the final output notification. The system is divided into two primary nodes: the transmitter node, which is responsible for detecting vibrations and broadcasting data, and the receiver node, which processes the incoming signals to trigger the warning system. This architecture ensures that information is transmitted over long distances reliably using the LoRa protocol, while the Wi-Fi integration allows for seamless data management and monitoring, shown in Fig. 1.

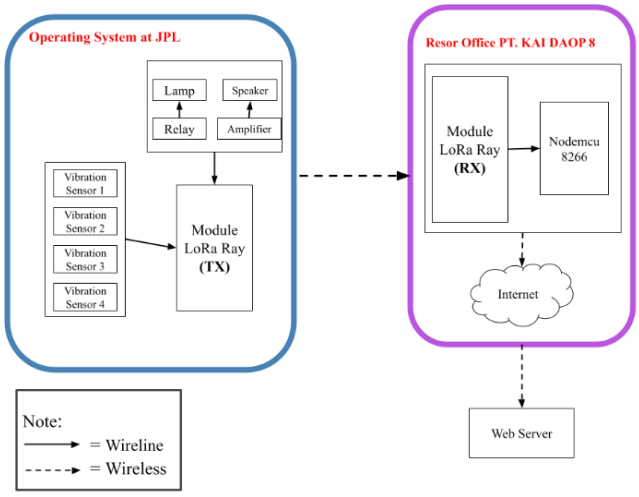

Figure 1. Diagram System

C. Materials and Methods

The research was conducted using a specific set of hardware components designed to meet the system requirements. These components were integrated to ensure the reliability and functionality of the proposed system, as detailed in the Table I below.

TABLE I
MATERIALS WITH THEIR FUNCTION

No.	Component	Brief Description
1.	LoRa Ray Module	System controller and RF transceiver (Tx/Rx)
2.	SW-420 Vibration Sensor	Detects object presence via mechanical vibrations
3.	Power Supply	24V DC voltage source for the system
4.	Audio Amplifier	Amplifies audio signals for the output system
5.	Node MCU ESP8266	Wi-Fi gateway for IoT/Internet connectivity
6.	2-Channel Relay	Switches and controls high-power peripherals
7.	LED Indicator	Provides visual status output
8.	Loudspeaker	Provides audio notification output
9.	Push Button	Manual input trigger for system activation

The materials utilized in this study consist of an integrated hardware-software framework. Key hardware components include a LoRa Ray module for long-range communication, an SW-420 sensor for vibration detection, and a Node MCU ESP8266 for internet connectivity. The complete technical specifications for system implementation are summarized in Table 1. The complete system architectures are illustrated in Fig. 2 and Fig. 3, that showing the integration between the Level Crossing (JPL) as the transmitter and the PT. KAI DAOP 8 Surabaya Resort Office as the receiver. The figure also details the power source points and the overall circuit configuration.

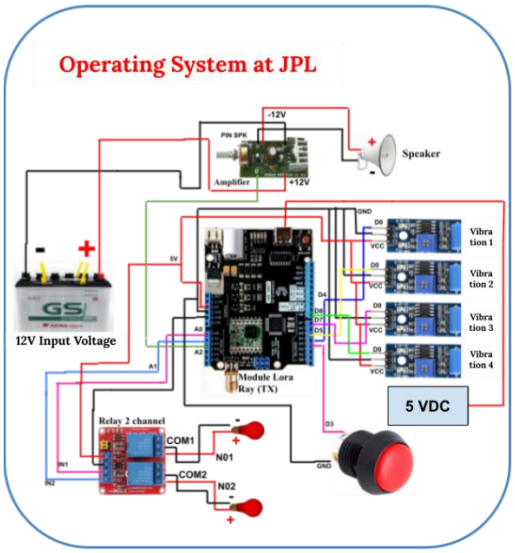

Figure 2. Circuit Schematic Transmitter

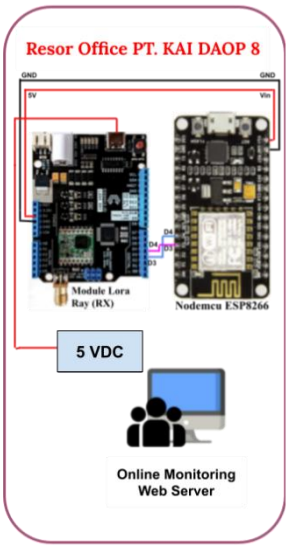

Figure 3. Circuit Schematic Receiver

The specific pin assignments and hardware configurations for the system components are detailed in Table II. This table outlines the electrical interconnections necessary for the integrated functionality of the entire system.

TABLE II
SOURCE AND DESTINATION

No.	Source Pin	Destination Pin
1	12V Power Supply (+)	Amplifier (+12V)
2	12V Power Supply (-)	Amplifier (-12V)
3	Amplifier Speaker Out (+)	Speaker Terminal (+)
4	Amplifier Speaker Out (-)	Speaker Terminal (-)
5	LoRa Ray Digital Pin A2	Amplifier Input Pin
6	5V Power Supply	LoRa Ray USB Pin
7	Vibration Sensors GND (1, 2, 3, 4)	LoRa Ray (TX) GND
8	Vibration Sensors VCC (1, 2, 3, 4)	LoRa Ray (TX) 5V
9	Vibration Sensor 1 D0 Pin	LoRa Ray (TX) D4
10	Vibration Sensor 2 D0 Pin	LoRa Ray (TX) D5
11	Vibration Sensor 3 D0 Pin	LoRa Ray (TX) D7
12	Vibration Sensor 4 D0 Pin	LoRa Ray (TX) D8
13	Push Button (+)	LoRa Ray (TX) D3
14	Push Button (-)	LoRa Ray (TX) GND
15	Relay Pin COM1	LED 1 Cathode (-)
16	Relay Pin COM2	LED 2 Cathode (-)
17	Relay Pin NO1	LED 1 Anode (+)
18	Relay Pin NO2	LED 2 Anode (+)
19	LoRa Ray (RX) D3	ESP8266 D4
20	LoRa Ray (RX) D4	ESP8266 D3
21	LoRa Ray 5V Pin	ESP8266 Vin
22	LoRa Ray (RX) GND	ESP8266 GND
23	5V Power Supply	LoRa Ray (RX) USB Pin

III. RESULTS AND DISCUSSION

A. *Result of Tool Design*

Detection node is a critical component of the level crossing safety system, designed to detect and provide early notification regarding train arrivals and departures. Strategically positioned at the nearest Level Crossing (JPL) post, this node serves as the primary field sensing unit. The next stage involved testing the LoRa communication performance between the node and the server. This testing was conducted at Surabaya Gubeng Station, which served as the primary site for data collection and research. The test scenario focused on evaluating the impact of distance on data transmission efficiency. The final hardware implementation of the detection node and the server circuit are illustrated in Fig. 4 and Fig. 5.

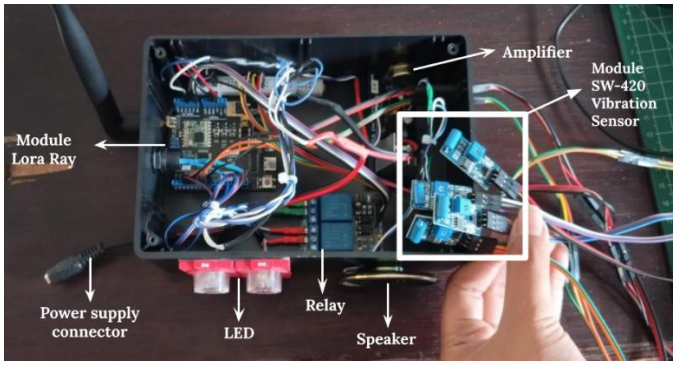

Figure 4. Detection Node Circuitry

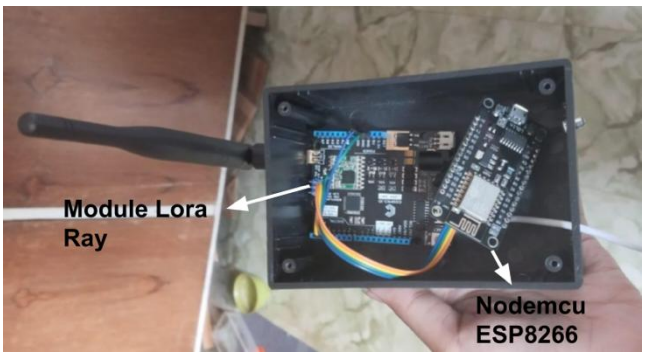

Figure 5. Server Node Circuitry

Circuitry component installation is shown in figure 4 and figure 5. For detection consists module LoRa Ray TX, a connector, a LED 12 Volt DC, a relay 2 channels, a speaker, a vibration sensor SW-420, and Amplifier. The sensor consists 4 sensors for difference place. For server circuit consists module Lora Ray RX and Nodemcu ESP8266. The system architecture consists of a transmitter node and a receiver node, both utilizing the LoRa Ray module, which integrates an ATmega-based microcontroller with a LoRa antenna for streamlined hardware implementation.

On the transmitter side, the microcontroller manages four vibration sensors, a 2-channel relay, and an audio amplifier. When a vibration sensor detects a train's arrival or departure on a specific track, the system triggers the 2-channel relay to activate constant flip-flop LED indicators and powers the amplifier to drive a loudspeaker, emitting tones generated via the Arduino IDE. Simultaneously, the transmitter broadcasts time-stamped arrival or departure data wirelessly to the receiver node. Upon receiving the signal, the receiver-side LoRa Ray module transfers the data to a NodeMCU ESP8266, which acts as a Wi-Fi gateway to upload the information to a web server. This data is then stored and displayed on a web application, allowing authorized station personnel and crossing guards to monitor train movements in real-time through a secure login interface.

B. Web Server

Based on the test results, the web application for the crossing safety system development is designed with two primary user access levels: Admin and Staff. The platform provides essential features, including a secure login gateway, a dashboard for a general system overview, and a user management module. Furthermore, it records real-time data on train arrival and departure times, all of which can be exported and downloaded to support reporting and administrative requirements.

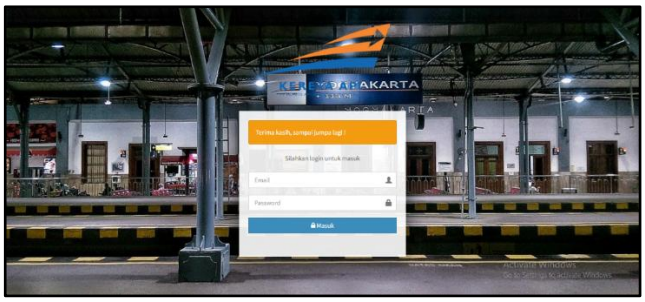

Figure 6. Login Page

The login page shown in Fig. 6 ensures secure access to the system. Users must input their credentials to proceed. A successful login grants access to the home dashboard, while invalid entries trigger an error notification to inform the user of the failed attempt.

Figure 7. Landing Page

The dashboard shown in Fig. 7 is the main landing page after authentication. It features the company logo as a brand identity and provides a brief profile of the company, including its geographical location.

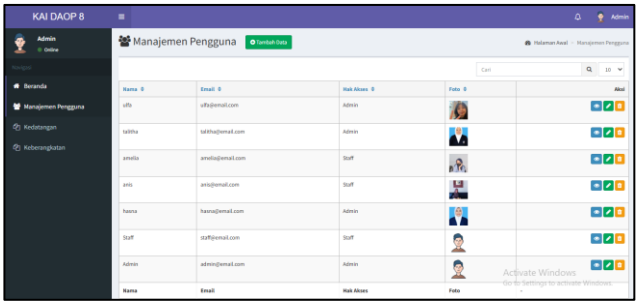

Figure 8. User Management Page

Fig. 8 illustrates the User Management page, which functions to manage registered user data within the system. This interface displays comprehensive user information, including full names, email addresses, access levels, and profile pictures. Additionally, it provides administrative controls for user data management, such as adding new users, viewing detailed profiles, editing existing information, and removing users from the system.

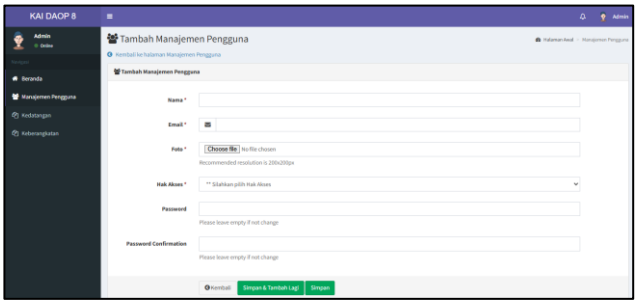

Figure 9. Add User Page

Fig. 9 illustrates the 'Add User' feature, which provides a dedicated interface for registering new personnel into the system. This form includes several essential input fields that must be completed to ensure a valid registration. Required information includes the user's full name, a valid email address for account identification, a profile photograph for visual recognition, and a secure password for system authentication.

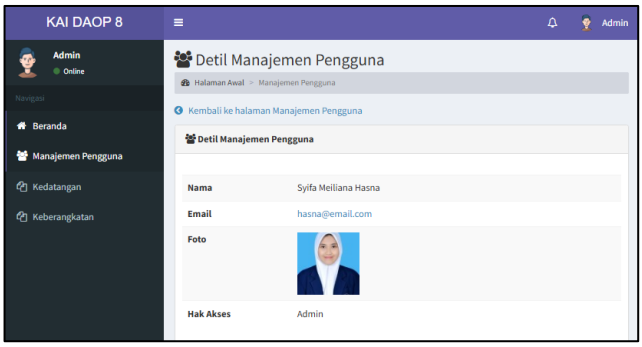

Figure 10. Detail User

The detailed view of user data is shown in Fig. 10. It retrieves and displays all registered account attributes, such as name, email, profile image, and user roles. This feature allows administrators to verify the complete profile of each user within the system efficiently.

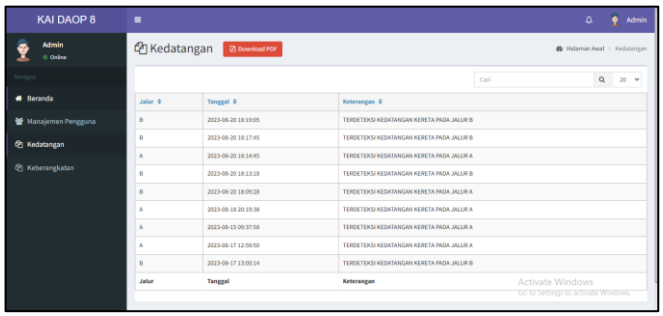

Figure 11. Arrival Monitoring Page

The Arrival Data interface is illustrated in Fig. 11. This page captures and visualizes the arrival timestamps transmitted from the detection nodes.

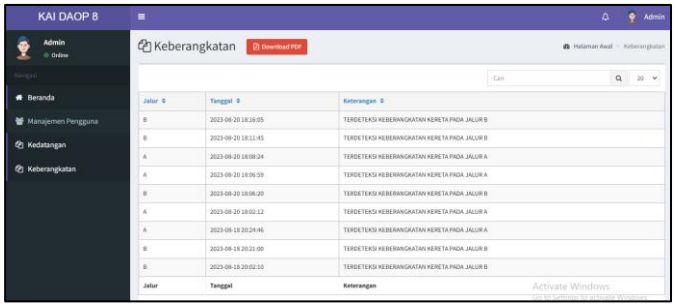

Figure 12. Departure Monitoring Page

Fig. 12 illustrates the Train Departure interface, which displays a detailed log of detected activities. The information provided includes the specific rail track, the precise date and time of the event, and the activity status triggered upon train detection. Furthermore, this menu is equipped with a data export feature, allowing users to download activity files

C. *Tool Test Results*

The testing phase of this research utilized a digital vibration meter as a reference tool to measure the vibration intensity generated by train movements. This measurement process was conducted to validate the data acquired by the sensor nodes, as illustrated in Fig. 13 below.

Figure 13. Testing with Vibration Meter

The measurement procedure followed strict protocols for safety and accuracy: the vibration meter was set to velocity mode and operated under the supervision of PT KAI personnel. For safety, a 2-meter clearance was maintained while recording vibrations from trains passing over the instrumented rails (Table III)

TABLE III
VIBRATION METER TESTING

No	Distance (M)	Vibration Meter (kHz)	Vibration Meter Conversion (kHz)	% Error
1	2	0,16	0,129748	1,89%
2	2	0,19	0,130582	3,12%
3	2	0,2	0,13086	3,45%
4	2	0,22	0,131416	4,02%
5	2	0,28	0,133084	5,24%
6	2	0,26	0,132528	4,90%
7	2	0,33	0,134474	5,92%
8	2	0,38	0,135864	6,42%
9	2	0,35	0,13503	6,14%
10	2	0,41	0,136698	6,66%
Average Percentage Error				4,78%
Percentage Accuracy				95,22%

Field testing was conducted at Surabaya Gubeng Station by varying the distance between the transmitter and receiver to obtain accurate experimental data. The receiver coordinates were determined using Google Earth, with the detailed mapping points illustrated in Fig. 14.

Figure 14. Mapping Point in Google Earth

To test the LoRa transmission range, 11 sample points were mapped and recorded, the details of which are presented in Table IV.

TABLE IV
RESULT TESTING IN FIELD

No	Tx		Rx		Distance (m)	Status
	Latitude (-)	Longitude	Latitude (-)	Longitude		
1	7.268694	112.751647	7.267036	112.751878	187.5977	Succes
2	7.268694	112.751647	7.266772	112.751944	217.937	Succes
3	7.268694	112.751647	-7.2662	112.752064	283.3503	Succes
4	7.268694	112.751647	7.265778	112.7521	330.6877	Succes
5	7.268694	112.751647	7.264878	112.752206	432.1946	Succes
6	7.268694	112.751647	7.264297	112.752514	502.1613	Succes
7	7.268694	112.751647	7.263736	112.752628	566.3025	Succes
8	7.268694	112.751647	7.263231	112.752733	624.0923	Succes
9	7.268694	112.751647	7.262561	112.752861	700.5211	Succes
10	7.268694	112.751647	7.262033	112.752958	760.6691	Succes
11	7.268694	112.751647	7.261328	112.752797	835.4307	Fail

The testing results indicate that the maximum effective range achieved by the LoRa system is 760 meters. This limitation is due to the inverse relationship between distance and signal strength; as the distance between the transmitter and receiver increases, the received signal strength weakens. Several factors contributed to the transmission failure beyond this point, specifically the increased distance and the presence of numerous physical obstacles at the testing site. These obstacles interfered with the signal propagation quality, leading to data loss at longer ranges.

D. Quality of Service

Quality of Service (QoS) testing is a systematic process used to evaluate the service quality provided by a system to ensure optimal performance. QoS refers to the system's capability to meet specific requirements and expectations regarding service quality, reliability, and responsiveness. In accordance with the methodology outlined in Chapter III, this research requires a rigorous QoS evaluation. The testing was conducted over a single day across four distinct time intervals: morning, afternoon, evening, and night.

1) *Packet Loss*: Packet loss is a network performance metric used to assess the quality of a network by identifying the number of data packets that fail to reach their destination during the transmission process. A high percentage of packet loss indicates poor network quality, which can be attributed to several factors such as hardware malfunctions in network devices or network overloading (congestion).

Measurement	Captured	Displayed
Packets	1915	2 (0.1%)
Time span, s	86.906	6.755
Average pps	22.0	0.3
Average packet size, B	472	754
Bytes	904562	1508 (0.2%)
Average bytes/s	10 k	223
Average bits/s	83 k	1785

Figure 15. Detail Packet Loss

The percentage of packet loss is calculated using the following Equation (1):

$$Packet\ Loss = \left(\frac{package\ sent - package\ received}{package\ sent}\right) x\ 100 \quad (1)$$

Based on the previously mentioned equation, the calculation of the Packet Loss value for each time interval is as follows:

$$Packet\ Loss = \left(\frac{package\ sent - package\ received}{package\ sent}\right) x\ 100$$

$$= \left(\frac{1915 - 1913}{1915}\right) x100$$

$$= 0{,}00104\ x\ 100$$

$$= 0{,}104\%$$

The experimental results yielded an average packet loss of 0.104%. According to the TIPHON standardization, this performance is classified under the 'Very Good' category. The classification is based on the TIPHON scale, which defines 0%–3% as 'Very Good' (with sub-categories often refined as 0% for ideal and 1%–3% for good), 4%–15% as 'Fair' (Moderate), and values exceeding 25% as 'Poor'.

2) *Throughput:* is a network performance metric that measures the actual volume of data successfully transmitted or processed over a network within a specific period. It is quantified by calculating the amount of data sent or received per unit of time, typically measured in megabits per second (Mbps) or kilobits per second (kbps). A higher throughput value indicates faster data transmission and superior network performance. The following data represents the transmission and reception results, as illustrated in Fig. 16.

Measurement	Captured	Displayed
Packets	1915	1915 (100.0%)
Time span, s	86.906	86.906
Average pps	22.0	22.0
Average packet size, B	472	472
Bytes	904562	904562 (100.0%)
Average bytes/s	10 k	10 k
Average bits/s	83 k	83 k

Figure 16. Network Technical Details

using the following Equation (2):

$$Troughput = \left(\frac{packages\ received\ (bytes)}{transmission\ time\ (s)}\right) x\ 8 \quad (2)$$

Based on the network technical details illustrated in Fig. 16, the total number of packets received is 904,562. The following is the calculation for the throughput value:

$$troughput = \left(\frac{packages\ received\ (bytes)}{transmission\ time\ (s)}\right) x\ 8$$

$$= \left(\frac{904562}{86.902}\right) x\ 8$$

$$= 83{,}27191549101287\ bits\ x\ 1000000$$

$$= 83\ Mb$$

In conclusion, the network quality falls into the 'Very Good' throughput category, achieving an index of 4. It's refers to the TIPHON standardization, which categorizes performance into five levels: Very Good (Index 4), Good (Index 3), Fair (Index 2), Poor (Index 1), and Bad (Index 0).

3) Delay (also known as latency): is the measurement and evaluation of the time required for data to travel through the network from the transmitter to the receiver. The objective of delay testing is to ensure that the system's performance aligns with the specified timing requirements. Monitoring delay is critical, as it directly reflects the overall efficiency and impact of network performance on real-time data delivery. The delay value is obtained by calculating the difference between Time 2 and Time 1, as illustrated in Fig. 17 below.

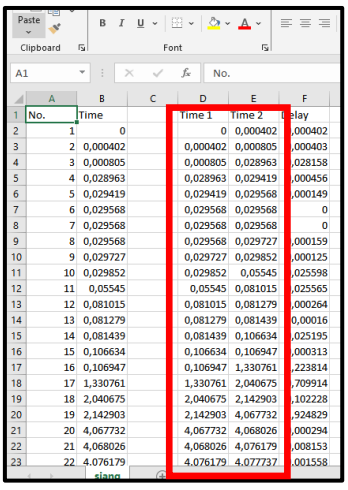

No.	Time	Time 1	Time 2	Delay
1	0	0	0,000402	,000402
2	0,000402	0,000402	0,000805	,000403
3	0,000805	0,000805	0,028963	,028158
4	0,028963	0,028963	0,029419	,000456
5	0,029419	0,029419	0,029568	,000149
6	0,029568	0,029568	0,029568	0
7	0,029568	0,029568	0,029568	0
8	0,029568	0,029568	0,029727	,000159
9	0,029727	0,029727	0,029852	,000125
10	0,029852	0,029852	0,05545	,025598
11	0,05545	0,05545	0,081015	,025565
12	0,081015	0,081015	0,081279	,000264
13	0,081279	0,081279	0,081439	,00016
14	0,081439	0,081439	0,106634	,025195
15	0,106634	0,106634	0,106947	,000313
16	0,106947	0,106947	1,330761	,223814
17	1,330761	1,330761	2,040675	,709914
18	2,040675	2,040675	2,142903	,102228
19	2,142903	2,142903	4,067732	,924829
20	4,067732	4,067732	4,068026	,000294
21	4,068026	4,068026	4,076179	,008153
22	4,076179	4,076179	4,077737	,001558

Figure 17. First and Second Time Stamps

The delay is obtained by subtracting Time 1 from Time 2. As illustrated in Figure 4.22, this calculation was performed using the spreadsheet formula =E2-D2, resulting in a value of 86.905595 s. Following this, the average delay must be calculated using the Equation 3 below:

$$Average\ delay = \frac{total\ delay}{total\ packet\ receivd} \quad (3)$$

$$= \frac{86{,}905595}{1915}$$

$$= 0{,}045381512\ s$$

$$= 45{,}38\ ms$$

The calculated average delay of 45.38 ms is classified as 'Very Good' with an index of 4, as it is below the 150 ms threshold. According to the TIPHON standardization, the delay categories are defined as follows: Very Good (Index 4) for delays less than 150 ms, Good (Index 3) for delays between 150 ms and 300 ms, Fair (Index 2) for delays between 300 ms and 450 ms, and Poor (Index 1) for delays exceeding 450 ms.

4) *Jitter:* is the measurement and evaluation of delay variation caused by network congestion or queuing delays, which can lead to an unresponsive transmission process. The measurement of jitter is similar to delay; however, it specifically focuses on the difference between the first delay value and the second delay value in a sequence of packets.

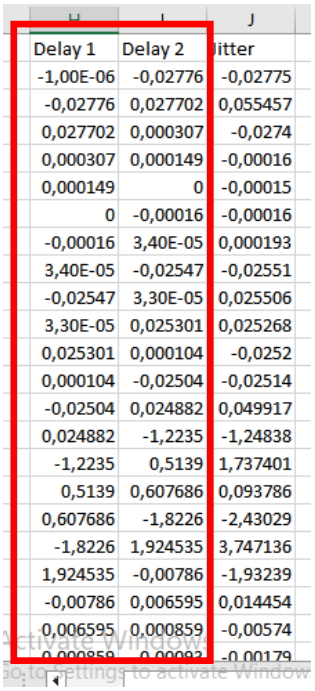

Delay 1	Delay 2	Jitter
-1,00E-06	-0,02776	-0,02775
-0,02776	0,027702	0,055457
0,027702	0,000307	-0,0274
0,000307	0,000149	-0,00016
0,000149	0	-0,00015
0	-0,00016	-0,00016
-0,00016	3,40E-05	0,000193
3,40E-05	-0,02547	-0,02551
-0,02547	3,30E-05	0,025506
3,30E-05	0,025301	0,025268
0,025301	0,000104	-0,0252
0,000104	-0,02504	-0,02514
-0,02504	0,024882	0,049917
0,024882	-1,2235	-1,24838
-1,2235	0,5139	1,737401
0,5139	0,607686	0,093786
0,607686	-1,8226	-2,43029
-1,8226	1,924535	3,747136
1,924535	-0,00786	-1,93239
-0,00786	0,006595	0,014454
0,006595	0,000859	-0,00574
0,000859	0,00093	-0,00179

Figure 18. First and Second Delay

Jitter is obtained by calculating the difference between Delay 2 and Delay 1. As shown in Figure 18, this was performed using the formula =I2-H2, resulting in a jitter value of 0.05086 s

between the two delays. Subsequently, the average jitter must be determined using the following equation:

$$Average\ jitter = \frac{total\ jitter}{packet\ received - 1}$$

$$= \frac{0{,}05086}{1914} = 2{,}6572622\ s = 0{,}026\ ms$$

The calculated average jitter of 0.026 ms is classified as 'Good' with an index of 3, as the value falls within the 0 ms – 75 ms range. According to the TIPHON standardization, the jitter categories are defined as follows: Very Good (Index 4) for a jitter of 0 ms, Good (Index 3) for jitter between 0 ms and 75 ms, Fair (Index 2) for jitter between 75 ms and 125 ms, and Poor (Index 1) for jitter between 125 ms and 225 ms.

The descriptions provided above outline the calculation methods for Quality of Service (QoS) for each parameter, specifically Packet Loss, Throughput, Delay, and Jitter. The following results present the comprehensive QoS evaluation obtained from the experimental testing, in Table V.

TABLE V
SUMMARY OF QOS EVALUATION RESULTS

Parameter	Value	Quality
Packet Loss (%)	0,1	Very Good
Throughput (Mbps)	83	Very Good
Delay (ms)	45,38	Very Good
Jitter (ms)	0,026	Good

IV. CONCLUSION

This research successfully developed a vibration-based train monitoring system integrated with a functional web-based management interface. Experimental results demonstrate that the web application effectively manages user credentials and provides real-time monitoring of train activities with an automated reporting feature. Furthermore, field testing at Surabaya Gubeng Station established that the LoRa-based communication system maintains a reliable transmission range up to 760 meters, though performance is eventually limited by signal propagation issues and physical obstacles at greater distances. Ultimately, this system offers a practical and efficient solution for enhancing level-crossing safety and streamlining administrative reporting for railway personnel.

V. ACKNOWLEDGEMENTS

The authors would like to express their sincere gratitude to PT Kereta Api Indonesia (Persero), specifically the personnel at Surabaya Gubeng Station, for providing technical guidance and safety supervision during the field-testing phase. We also extend our appreciation to the Department Electrical Engineering at the State Polytechnic of Malang for supporting this research. Furthermore, the authors are very much open to constructive criticism, suggestions, and corrections from reviewers to improve the quality and accuracy of this research in the future.

VI. REFERENCE

[1] D. S. Oktaria, F. L. Desei, and A. Darmawan, "Kajian Lalu-Lintas di Perlintasan Sebidang Resmi Tidak Dijaga Jalan Raya Beji dan Jalan Yonkav Kabupaten Pasuruan," Jurnal Kacapuri, vol. 4, no. 2, pp. 296–308, 2021.

[2] R. I. Borman, K. Syahputra, and P. Prasetyawan, "Implementasi Sistem Kendali Palang Pintu Kereta Api Berbasis Mikrokontroler," in Seminar Nasional Teknik Elektro, Batu, Malang, 2018.

[3] B. P. Pangestu, B. P. Prasetio, and G. E. Setyawan, "Implementasi Kendali Palang Pintu Kereta Api Menggunakan IR Sensor dan NRF24L01," Jurnal Pengembangan Teknologi Informasi dan Ilmu Komputer, vol. 1, no. 4, pp. 282–291, 2017.

[4] N. Costrada and H., "Rancang Bangun Sistem Peringatan Dini pada Perlintasan Kereta Api Berbasis Sensor Serat Optik dan Transceiver nRF24L01+," Jurnal Fisika Unand, vol. 8, no. 3, pp. 234–239, 2019.

[5] Hartono, "Perlintasan Sebidang Kereta Api di Kota Cirebon," Jurnal Penelitian Transportasi Darat, vol. 18, no. 1, pp. 45–62, 2018.

[6] F. Alviandi, K. Koesmarijanto, and H. Darmono, "Perancangan dan Analisa Antena Yagi 12 Elemen untuk Module LoRa RFM95W pada Frekuensi 915 MHz," Journal of Telecommunication Network (Jurnal Jaringan Telekomunikasi), vol. 11, no. 1, pp. 44–49, 2021, doi: 10.33795/jartel.v11i1.34.

[7] B. P. Manullang, Y. Saragih, and R. Hidayat, "Implementasi NodeMCU ESP8266 dalam Rancang Bangun Sistem Keamanan Sepeda Motor Berbasis IoT," JIRE (Jurnal Informatika & Rekayasa Elektronika), vol. 4, no. 2, pp. 163–170, 2021.

[8] M. Kusriyanto and N. Wismoyo, "Sistem Palang Pintu Perlintasan Kereta Api Otomatis dengan Komunikasi Wireless Berbasis Arduino," Teknoin, vol. 23, no. 1, pp. 73–80, 2017.

[9] S. Turangga, M., and Y. A., "Analisis Kualitas Jaringan Internet Menggunakan Parameter Quality of Service pada Alfamart Tuparev 70," Jurnal Mahasiswa Teknik Informatika, vol. 6, no. 1, pp. 392–398, 2022.

[10] M. A. S. Arifin, R. Pebriansyah, and B. Santoso, "Prototipe Penerapan Internet of Things pada Sistem Informasi," Jurnal Sustainable: Jurnal Hasil Penelitian, vol. 8, no. 2, pp. 83–89, 2019.

[11] M. Kusriyanto and N. Wismoyo, "Sistem Palang Pintu Perlintasan Kereta Api Otomatis dengan Komunikasi Wireless Berbasis Arduino," Teknoin, vol. 23, no. 1, pp. 73–80, 2017.

[12] B. P. Pangestu, B. P. Prasetio, and G. E. Setyawan, "Implementasi Kendali Palang Pintu Kereta Api Menggunakan IR Sensor dan NRF24L01," Jurnal Pengembangan Teknologi Informasi dan Ilmu Komputer, vol. 1, no. 4, pp. 282–291, 2017.

[13] M. Kusriyanto and N. Wismoyo, "Sistem Palang Pintu Perlintasan Kereta Api Otomatis dengan Komunikasi

Wireless Berbasis Arduino," Teknoin, vol. 23, no. 1, pp. 73–80, 2017.

[14] N. A. S. Putri, M. D. Atmadja, and K. Koesmarijanto, "Implementation of Data Collection and Payment Control Systems Automatically Using Android Based QR Code," Journal of Telecommunication Network (Jurnal Jaringan Telekomunikasi), vol. 13, no. 1, 2023.

[15] S. Firdaus, "Analysis of LoRaWAN Network Signal Coverage and Quality Parameters in Real-Time: Case Study of Cikumpa River Water Quality Monitoring, Depok City," Teknika, vol. 13, no. 2, 2024.